International Journal of Pharmaceutics 625 (2022) 122140

Contents lists available at ScienceDirect

International Journal of Pharmaceutics

journal homepage: www.elsevier.com/locate/ijpharm

Development of combi-pills using the coupling of semi-solid syringe extrusion 3D printing with fused deposition modelling

Bin Zhang [a], Xin Yi Teoh [b], Jiongyi Yan [c], Andrew Gleadall [c], Peter Belton [d], Richard Bibb [e], Sheng Qi [a,*]

[a] School of Pharmacy, University of East Anglia, Norwich, UK
[b] School of Pharmaceutical Sciences, Universiti Sains Malaysia, Penang, Malaysia
[c] School of Mechanical, Electrical and Manufacturing Engineering, Loughborough University, Loughborough, UK
[d] School of Chemistry, University of East Anglia, Norwich, UK
[e] School of Design and Creative Arts, Loughborough University, Loughborough, UK

ARTICLE INFO

Keywords:
Controlled drug delivery
Combi-pill
syringe based extrusion 3D printing
Fused deposition modelling

ABSTRACT

Three-dimensional (3D) printing allows for the design and printing of more complex designs than traditional manufacturing processes. For the manufacture of personalised medicines, such an advantage could enable the production of personalised drug products on demand. In this study, two types of extrusion-based 3D printing techniques, semi-solid syringe extrusion 3D printing and fused deposition modelling, were used to fabricate a combi-layer construct (combi-pill). Two model drugs, tranexamic acid (water soluble, rapid release) and indomethacin (poorly water-soluble, extended release), were printed with different geometries and materials compositions. Fourier transform infrared spectroscopy results showed that there were no interactions detected between drug-drug and drug-polymers. The printed combi-pills demonstrated excellent abrasion resisting properties in friability tests. The use of different functional excipients demonstrated significant impact on *in vitro* drug release of the model drugs incorporated in two 3D printed layers. Tranexamic acid and indomethacin were successfully 3D printed as a combi-pill with immediate-release and sustained-release profiles, respectively, to target quick anti-bleeding and prolonged anti-inflammation functions. For the first time, this paper systematically demonstrates the feasibility of coupling syringe-based extrusion 3D printing and fused deposition modelling as an innovative platform for various drug therapy productions, facilitating a new era of personalised combi-pills development.

1. Introduction

Polypills and combi-pills are pharmaceutical solid dosage forms that combine more than one medication into one single dose unit (Baumgartner et al., 2020; Khaled et al., 2015). The therapeutic rationale of these is to reduce the patient's 'pill burden', thus improve adherence and compliance to the treatment (Crossan et al., 2018; Roshandel et al., 2019; Group, 2011; Reardon, 2011; Wald et al., 2012). Most polypill products available for clinical use are fixed dose combinations for preventing or treating cardiovascular diseases (CVD) (Thom et al., 2014). Thus, in this study the term 'combi-pill' is used instead of 'polypill', one of the reasons is because we have a combination of two model drugs rather than many, so it does not fit the definition of 'poly-pill' yet. Another reason is to avoid confusion and highlight the fact that such an approach can be widely used to treat any conditions in which the patient's compliance could be improved by combining more than single-dose medications into a once-a-day single unit solid dose. Current large batch manufacturing methods are capable of producing polypills in either capsule (filled in mini-tablets) or tablet formats (Khaled et al., 2015; Robles-Martinez et al., 2019; Pereira et al., 2019; Haring et al., 2018; Tamargo et al., 2015) (Fig. 1a, b). However, the flexibility in dose adjustment tailored to individual patients needs is not possible with current large batch manufacturing methods and there is currently no product being commercially exploited for treating conditions other than CVD.

3D printing continues to attract increasing attention in the pharmaceutical science community due to its potential for flexibility and customizability in personalised medicine compared to traditional

* Corresponding author.
E-mail address: sheng.qi@uea.ac.uk (S. Qi).

https://doi.org/10.1016/j.ijpharm.2022.122140
Received 21 July 2022; Received in revised form 20 August 2022; Accepted 21 August 2022
Available online 27 August 2022

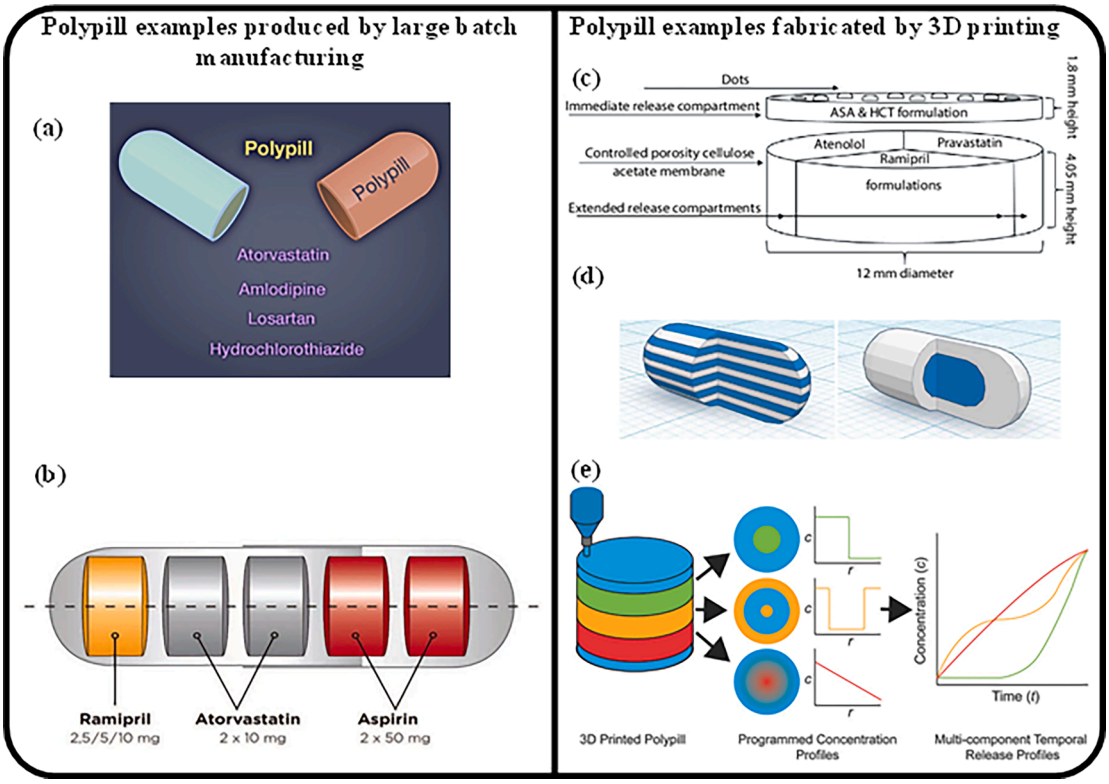

Fig. 1. (a) A polypill-based strategy for cardiovascular prevention (Muñoz et al., 2019); (b) The Fuster-CNIC-Ferrer CV Polypill (Trinomia®, Sincronium®, Iltria ®) technology (Tamargo et al., 2015); (c) Schematic structural diagram of the 3D printing of polypill design, showing the aspirin and hydrochlorothiazide immediate release compartment and atenolol, pravastatin, and ramipril sustained release compartments (Khaled et al., 2015); (d) 3D designs of the printlets – alternated layers design (left) and cone-shell design (right) (Goyanes et al., 2015); (e) Schematic concept of programming temporal release profiles of individual actives from a single polypill by controlling their spatial distributions (Haring et al., 2018).

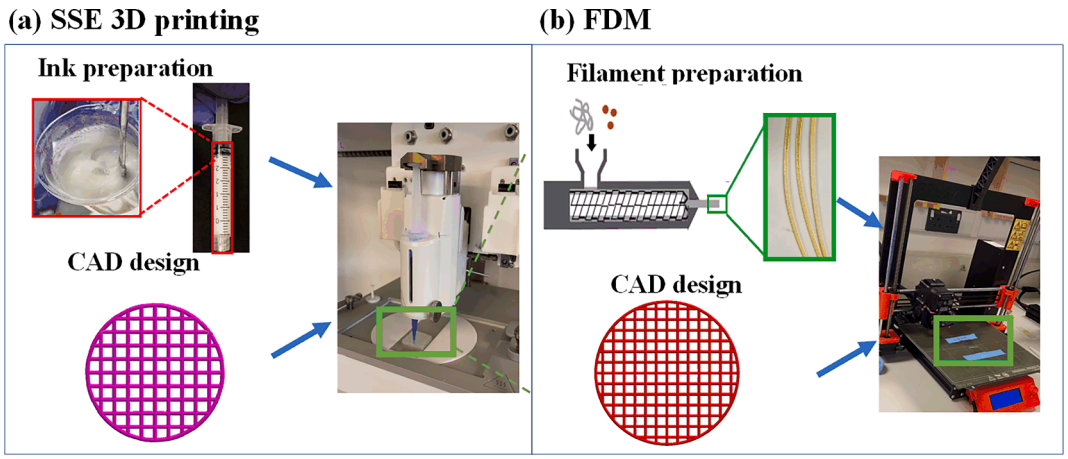

Fig. 2. (a) Schematic of using semi-solid syringe extrusion (SSE) 3D printing technique and (b) Hot melt extrusion filament and fused deposition modelling (FDM).

pharmaceutical manufacturing techniques (Hsiao et al., 2018; Wening and Breitkreutz, 2011). It offers the possibility of small batch manufacturing at, or close to, the point of care for patients who may benefit from combi-pill treatments (Khaled et al., 2015; Robles-Martinez et al., 2019; Pereira et al., 2019; Haring et al., 2018). Several 3D printing techniques have been applied in pharmaceutical research, such as stereolithography (Crossan et al., 2018, Roshandel et al., 2019), selective laser sintering (Group, 2011), inkjet printing (Reardon, 2011; Wald et al., 2012), and material extrusion-based 3D printing (Thom et al., 2014; Robles-Martinez et al., 2019; Pereira et al., 2019; Haring et al., 2018). The main 3D printing methods that have been explored for producing polypills are thermoplastic material extrusion, also known as fused deposition modelling or FDM (Goyanes et al., 2015; Zhang et al., 2021e; Zhang et al., 2021c), semi-solid syringe extrusion (Khaled et al., 2015; Zhang et al., 2022) and stereolithography (SLA) (Robles-Martinez et al., 2019; Crossan et al., 2018) (Fig. 1 c–e). Khaled et al. (2015) designed a polypill containing aspirin, hydrochlorothiazide, pravastatin, atenolol, and ramipril, a combination of drugs used to treat

Table 1
(a) HPMC based ink formulation and (b) Eudragit RL/indomethacin-based filament formulation.

a. HPMC based ink formulation

	Polymer	Additives		API
Ink name[a]	HPMC (w/v)	PVP (w/v)	CMC(w/v)	TXA (w/v)
15HPMC + 20PVP	15 %	20 %	–	–
15HPMC + 20PVP + 45TXA	15 %	20 %	–	45 %
15LHPMC + 20PVP	15 %	20 %	–	–
15LHPMC + 20PVP + 45TXA	15 %	20 %	–	45 %
10HPMC + 25PVP	10 %	25 %	–	–
10HPMC + 25PVP + 45TXA	10 %	25 %	–	45 %
35PVP + 45TXA	–	35 %	–	45 %
20PVP + 15CMC + 45TXA	–	20 %	15 %	45 %
20PVP + 10CMC + 60TXA	–	20 %	10 %	60 %

b. Eudragit RL/indomethacin-based filament formulation

Filament name	Eudragit RL (w/w)	Tween 80 (w/w)	PEG 4000 (w/w)	PEO (w/w)	Indomethacin (w/w)
Eudragit RL	100 %	–	–	–	–
Eudragit RL/IND/plasticisers	50 %	10 %	10 %	20 %	10 %

[a] The molecular weight of HPMC is circa 40 times higher than LHPMC The weight-to-volume (w/v) ratio is expressed as the ratio of the weight of material added to a fixed volume of water.

cardiovascular disease. As shown Fig. 1 c, these pills were printed by semi-solid syringe extrusion-based 3D printing at room temperature. The polypill had an immediate release compartment with aspirin and hydrochlorothiazide and three sustained release compartments containing pravastatin, atenolol, and ramipril. The drug release studies of the polypills demonstrated the intended immediate and sustained release profiles of different model drugs. Goyanes et al. (2015) used FDM to manufacture tablets containing paracetamol and caffeine. In order to obtain diverse drug release profiles, tablets with two different designs were 3D printed. As shown Fig. 1 d, the first design featured alternated layers of caffeine and paracetamol. While the second design, named DueCaplets, is a core–shell shaped caplet consisting of a core with one drug inside of an outer shell layer where the other drug was loaded. Results demonstrated a simultaneous release of both drugs within the model featuring alternate layers, whereas the DuoCaplets model showed release of the drug located at the outer layer followed by the drug located at the core of the capsule.

The combined use of more than one 3D printing method has not been reported to the best of our knowledge. Here we report the proof-of-principle results of the combined used of FDM and semi-solid syringe extrusion (SSE) 3D printing methods to produce combi-pills with two different APIs. SSE 3D printing has the potential advantage of allowing room-temperature deposition of semi-solid materials, often referred to as an ink, to build complex architectures, which offers the ability to process materials containing temperature-sensitive components (Zhang et al., 2020b; Tan et al., 2018; Zhang et al., 2020a) Both SSE 3D printing and FDM methods have been widely reported for the fabrication of pills, implants, and other medical devices using drug-polymer mixtures (Alhijjaj et al., 2016; Alhijjaj et al., 2019). SSE and FDM 3D printers can be relatively low-cost, bench-top, with small spatial footprints, low power requirements and portable with excellent potential to be modified for point of care manufacturing (Auriemma et al., 2022; Azad et al., 2020).

The two model drugs selected for this study are tranexamic acid (TXA) (highly water soluble, rapid release) and indomethacin (IND) (poorly water-soluble and extended release). Tranexamic acid is also a thermal- and photo-liable drug that requires high dose usage. This study aims to use it as a model drug to develop alternative printing solution for such drugs. The combi-pill was designed as a two-layer construct with the TXA-based layer on the top and the IND layer on the bottom. The advantage of the combi -pill is that only one pill needs to be taken instead of two, and such a combi-pill may be suitable for emergency situations such battlefield injuries or in natural disasters. TXA is a water-soluble antifibrinolytic that prevents or reduces bleeding by impairing fibrin dissolution and allow blood to clot (Huebner et al., 2017). In the treatment of wounded patient TXA should dissolve and be absorbed rapidly. Therefore, an immediate release layer consisting of TXA and hydroxypropyl methylcellulose were printed by SSE 3D printing. IND is a poorly soluble nonsteroidal anti-inflammatory drug (NSAID), in this case being used to reduce inflammation caused by injuries in a sustained manner (Nalamachu and Wortmann, 2014). Therefore, the IND layer of the combi-pill was formulated with Eudragit RL, this is widely used in controlled release formulation and was printed using FDM. Both TXA and IND layers were printed with various infill densities. The influence of geometrical design and material compositions of combi-pills and TXA and IND only pills on drug release rate was investigated. The method of preparing customised combi-pills with distinct release profiles presented in this study shows promising potential for the fabrication of patient-tailored personalised medicines.

2. Materials and methods

2.1. Materials

For syringe-based extrusion the materials used were: Hydroxypropyl methylcellulose (HPMC) (METOLOSE® SR 90SH-4000); LHPMC (METOLOSE® 90SH-100SR) (both donated by Shin-Etsu Chemical Co. Ltd. Tokyo, Japan; Polyvinylpyrrolidone (PVP) which were received as generous gifts from BASF (Ludwigshafen, Germany) and Evonik (Darmstadt, Germany) respectively; Croscarmellose sodium (CMC) was purchased from Sigma-Aldrich (St. Louis, Missouri, United States). Tranexamic acid (TXA) was purchased from Molecula (Darlington, UK). Salicylaldehyde (SA), used as an agent for UV detection of the TXA, was purchased from Sigma-Aldrich (St. Louis, Missouri, United States).

For material extrusion, the materials were Polyethylene glycol 4000, poly(ethylene oxide) (Mw = 100,000 g/mol) and Tween 80 (purchased from Sigma-Aldrich, St. Louis, Missouri, United States); Eudragit RL (received as a generous gift from BASF Ludwigshafen, Germany); Indomethacin (IND) was purchased from Molekula (Darlington, UK).

2.2. Preparation of semisolid inks and hot melt extrusion (HME) filaments

Drug-loaded ink was formulated by dissolving 45–60 %w/v TXA in Milli-Q water (20 mL) by magnetic stirring at 200 rpm for 2 h at room temperature. HPMC and PVP were added at 15 %-20 %w/v respectively.

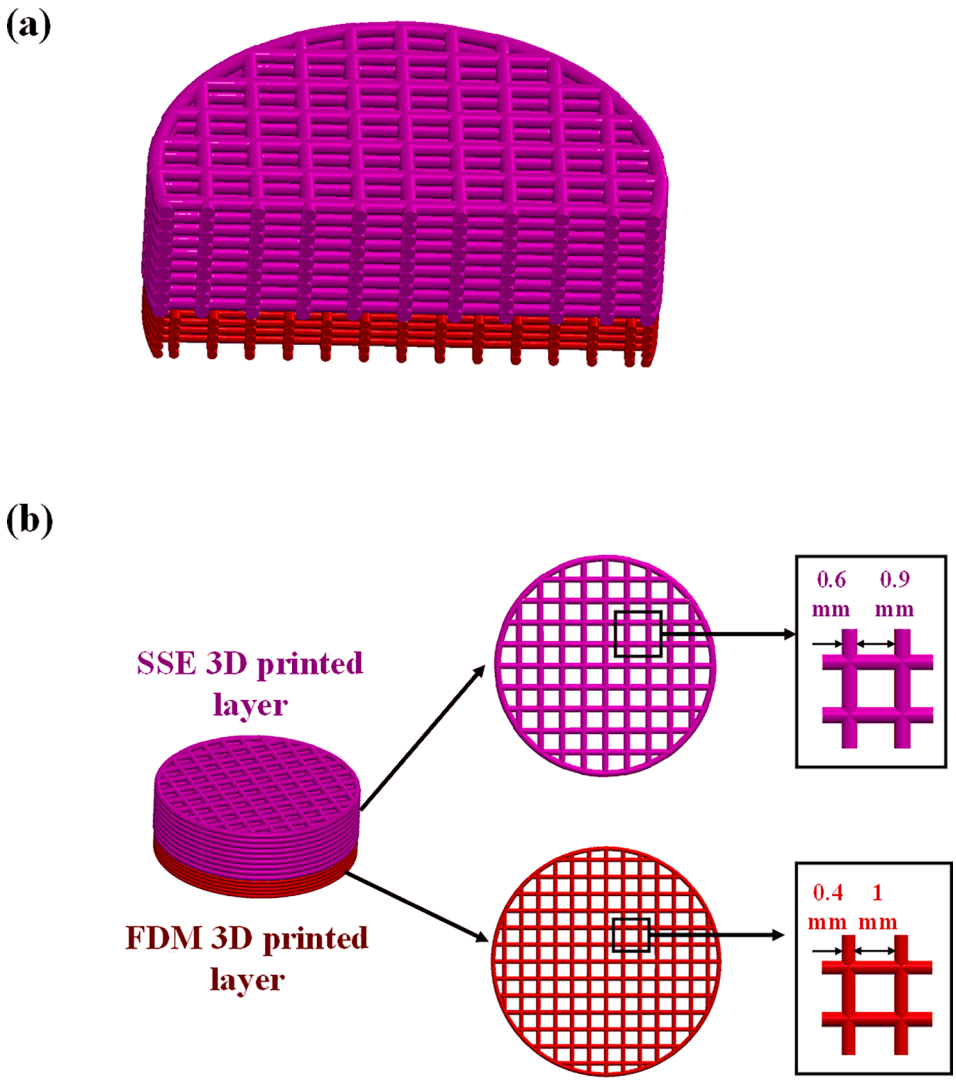

Fig. 3. (a) Combi-pill CAD model (zoomed-in cross-sectional view); (b) CAD design for SSE (SSE) 3D printing (top) and fused deposition modelling (FDM) (bottom). The SSE has 18 layers while the FDM has 5 layers in total.

10 %-15 %w/v of CMC was then added as an additive for ink formulation. The formulated inks were allowed to centrifuge at 4000 rpm for an hour to remove bubbles. Fig. 2a describes the SSE ink preparation and the details of the SSE ink formulations are shown in Table 1a. Material extrusion filaments were prepared from polymer, plasticizer and drug powders with amounts as shown in Table 1b) with a co-rotating twin screw Haake Minilab extruder (Thermo Fisher, Karlsruhe, Germany).

Fig. 2b describes the hot melt extrusion process for the filament manufacture. 5 g of materials (i.e., polymer, plasticizer and drug powder) were accurately weighted then physically mixed via mortar and pestle for 5 min and fed into to the Haake Minilab extruder. During the mixing stage of the materials in the extruder, the extrusion was performed at a screw speed of 100 rpm and a temperature of 100 °C, with 5 min circulation time to ensure homogeneity of the mixing. The 100 °C extrusion temperature was sufficient to fully melt the formulation without causing thermal degradation of IND. A circular die with a diameter of 1.75 mm and a screw speed of 100 rpm were used during the extrusion of the filament. The diameters of the filaments were measured using a digital calliper and the filaments' diameters were in the range of 1.75 ± 0.5 mm.

2.3. Design 3D constructs

3D constructs were designed for SSE 3D printing and FDM, separately. For the fabrication of combi-pills, both SSE printed and FDM printed tablets have the same diameter (20 mm) – the FDM print was done first, and the SSE was printed on top of it, as shown in the Fig. 3. The filament width of SSE 3D printed tablet was 0.6 mm, and its inter-filament distance was 0.9 mm, while the filament width of FDM 3D printed tablet was 0.4 mm and its inter-filament distance was 1 mm. The thickness of the tablets printed using SSE (TXA tablet layer) and FDM (IND tablet layer) was 5 mm and 1 mm, respectively. These thicknesses were used to ensure the drug contents of the combi-pill were similar to the doses used in clinic and commercially available tablets. The solid volume (V_{solid}) and surface area (SA_{solid}) of CAD models were generated using SolidWorks (Dassault Systèmes, Vélizy-Villacoublay, France). The SA/V was calculated as the value of the solid surface area to solid volume using Eq. (1).

$$SA/V = \left(\frac{SA_{solid}}{V_{solid}}\right) \quad (1)$$

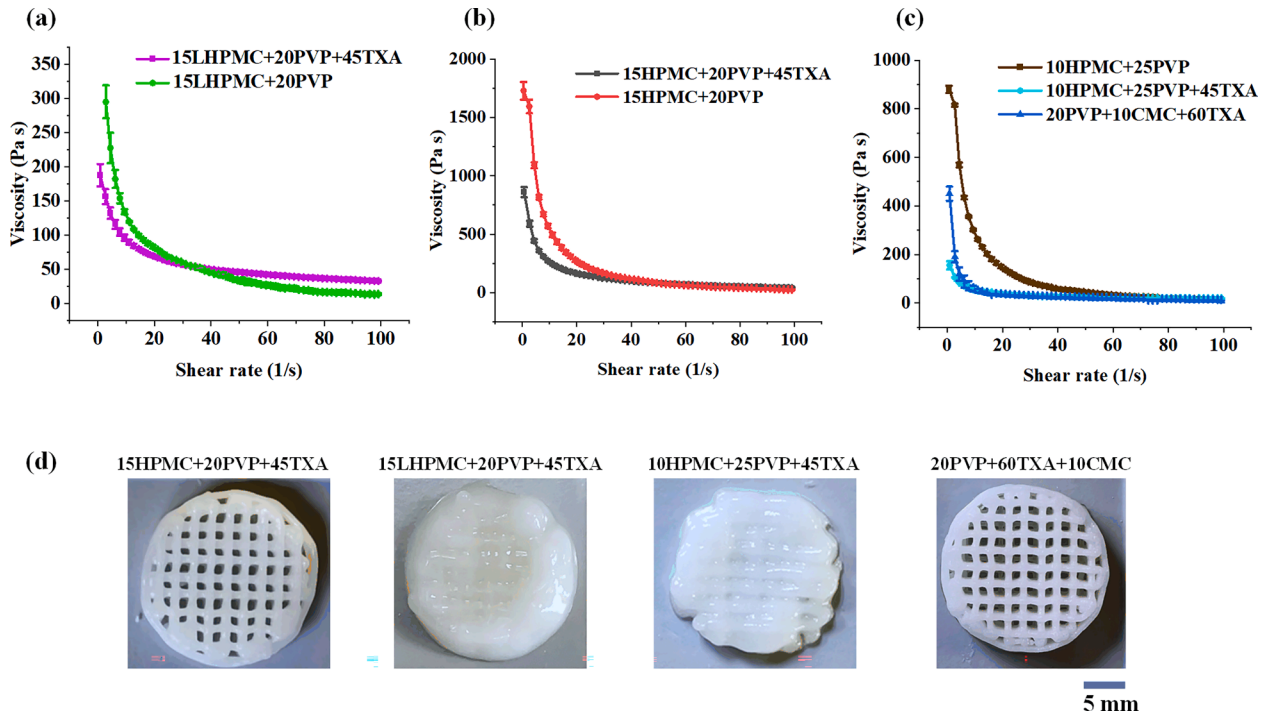

Fig. 4. Flow ramp viscosity of (a) LHPMC based inks with and without TXA; (b) HPMC based ink with and without TXA; (c) inks with and without adding HPMC (n = 3); (d) the visual appearances of SSE 3D printed tablets with different ink formulations and TXA drug loadings immediately after printing (prior to drying).

Table 2
Formulated inks viscosity and printability.

Ink name	Low-shear viscosity (Pa s) (n = 3)	Printability investigation
15HPMC + 20PVP	1728.5 ± 75.2	Not extrudable[a]
15HPMC + 20PVP + 45TXA	859.9 ± 44.0	Good for printing[b]
15LHPMC + 20PVP	283.2 ± 33.9	Too liquid for printing[c]
15LHPMC + 20PVP + 45TXA	188.1 ± 23.2	Merging issue[d]
10HPMC + 25PVP	880.4 ± 20.5	Failed for multi-layer printing[e]
10HPMC + 25PVP + 45TXA	155.4 ± 24.3	Merging issue[d]
20PVP + 10CMC + 60TXA	450.7 ± 41.3	Good for printing[b]

[a] The ink viscosity was too high to be force out through the nozzle.
[b] The ink was able to print the 18-layer circular structure without significant merging issue.
[c] The ink viscosity was too low to be not able to be print more than 5 layers.
[d] The ink was able to print the 18-layer circular structure without a significant merging issue.
[e] The extruded filament shape was not held, and it was not possible to print more than 5 layers.

2.4. 3D constructs fabrication with SSE and FDM

For combi-pill fabrication, the SSE component was printed on top of the FDM tablet. A piston driven SSE 3D printer (BioX, Cellink Life Sciences, Gothenburg, Sweden) was used to fabricate the 3D construct. The G-code of the design was generated in accordance with the predesigned CAD model. Each layer was comprised of parallel filaments with an average width of circa 600 μm, equivalent to the internal diameter (ID) of a 20 G nozzle. The SSE printing was implemented at room temperature (circa 21 °C) and both the printing nozzle and printing platform were not heated. The ink materials were extruded from an extrusion nozzle with an extrusion rate of 1–5 μL/s and a printing speed of 5–20 mm/s to obtain the filament diameter close to the nozzle diameter (600 μm). The drying process of the SSE printed tablet was investigated at three temperatures (25 °C, 37 °C and 60 °C). The FDM printer used in this study was Prusa i3 (Mk3S, Prague, Czech Republic). The nozzle diameter of the FDM printer used was 400 μm, stepper motors drive the motion in the Z direction via twin lead screws with an overall resolution of 0.001 mm/step with a 1.8° step angle. During printing, the nozzle temperature was set at 100 °C and the print platform was not heated. The whole printing process was performed at room temperature (21 °C). The extrusion rates from 0.1 to 0.2 mm/mm and printing speeds from 5.0 to 30.0 mm/s were investigated to optimize the 3D printing filament diameter as close to the nozzle diameter (400 μm) as possible. After the optimization process, the extrusion and printing rates of 0.15 mm/mm and 10 mm/s, respectively, were used for the FDM 3D printing. A glass slide was used as a collecting substrate on the print platform.

2.5. Rheological characterisation of SSE inks

Rheological measurements were conducted at 21 °C using a rheometer (Discovery HR30, TA Instruments, New Castle, Delaware, USA) with a cone-plate geometry. Continuous flow ramps were performed by varying the shear rate from 0.1 to 100 s^{-1}. Three replicates were taken for each ink.

2.6. FDM filament tensile test

The filament tensile test was performed using a Texture analyser (Stable Micro Systems, Surrey, UK) equipped with a 30 kg Load cell. Filaments were pulled axially with a tensile speed of 5 mm/minute. The tensile distance was set to 30 mm with a trigger force of 0.05 N and data was collected during both tensile and release. The fracture point is the filament break off point during the tensile test. The yield point was defined as the end of the linear stage. Texture analyser tests were done in triplicate for all tested filaments.

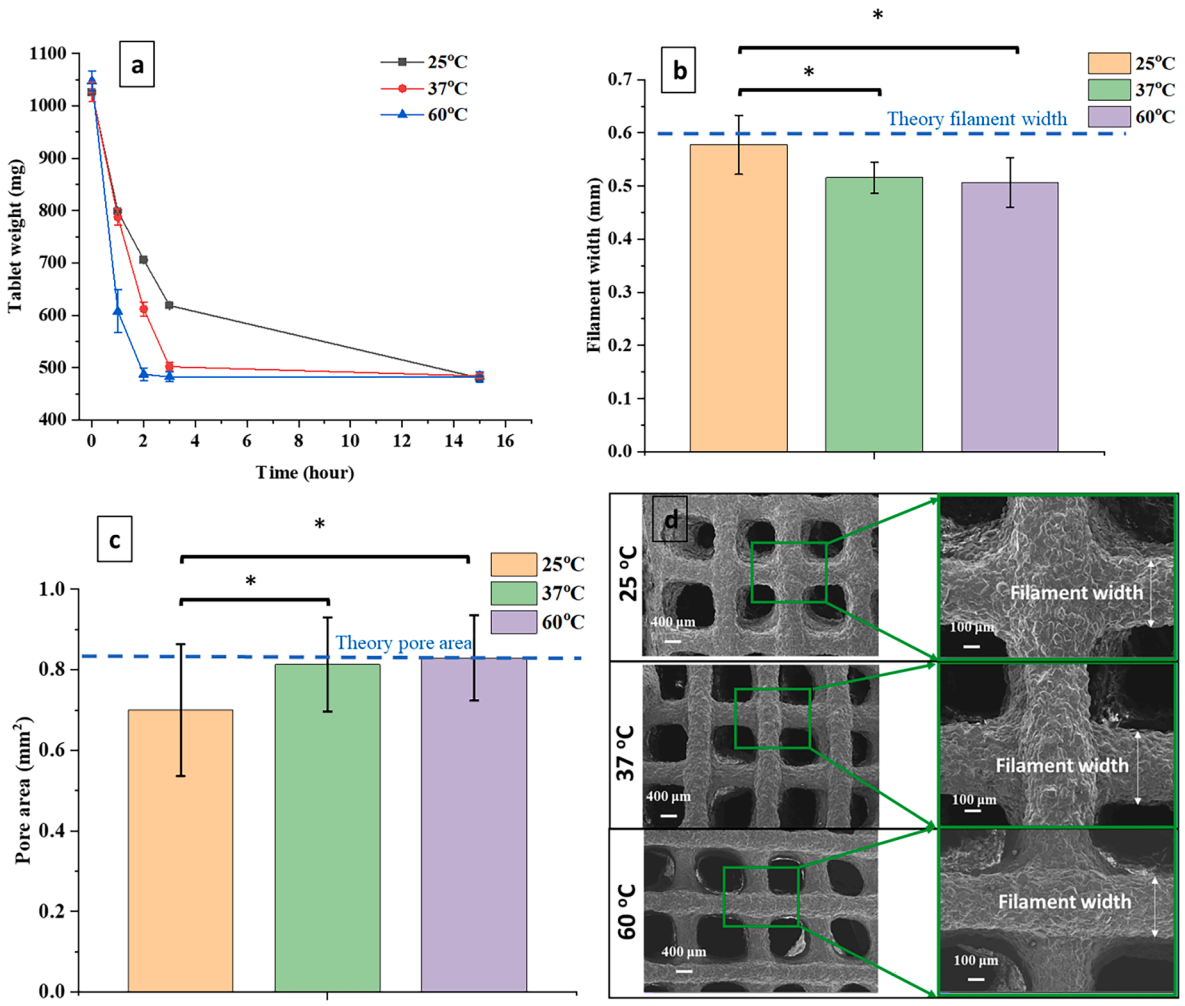

Fig. 5. (a) The influence of drying temperature on tablet weight, (b) filament width of the printed tablets, (c) tablet pore area and (d) SEM images of the tablets to illustrate the filament width and pore areas. All data were obtained from tablets dried for 48 h.

2.7. Shape fidelity analysis and surface morphology of 3D printed tablets

A FDSC196 light microscope (Linkam Scientific, Surrey, UK) was used to inspect the printed constructs. The extruded filament width was quantified by measuring at least 50 filaments using ImageJ software (https://rsb.info.nih.gov/ij/); the data was exported for analysis, and statistical distributions were plotted using Origin software 2018 (OriginLab Corporation, Northampton, Massachusetts, United States). The results were presented as the mean ± standard deviation. The filament width and pore area of the printed structures were measured in ImageJ software (Version 1.8.0, Bethesda, Maryland, USA). The measurements were repeated at 5 different sites on the sample. The data were plotted using Origin software (Version 2018, Northampton, Massachusetts, USA). Error bars represent the mean ± standard deviation. The surface morphology of the printed samples was evaluated using scanning electron microscopy (SEM) with a Zeiss Gemini 300 (Carl Zeiss AG, Oberkochen, Germany). The samples were first sputter-coated with gold. The images were taken at magnifications from ×25 to 200 with an acceleration voltage of 10 kV.

2.8. Physicochemical characterisation of 3D printed tablets

A Fourier transform infrared (FTIR) spectrophotometer (VERTEX 70, Bruker Optics, Ettlingen, Germany), equipped with a Golden Gate, Attenuated Total Reflectance (ATR) accessory (Specac Ltd., Orpington, United Kingdom) fitted with a diamond internal reflection element, was used to examine the raw materials and the prints. The spectra were collected over a wavenumber range of 500–4500 cm^{-1} with a resolution of 2 cm^{-1} at room temperature. All measurements were performed in triplicate.

2.9. Disintegration tests of 3D printed tablets

The disintegration process was implemented by putting the printed tablet in distilled water (25 mL) in a Petri dish and the disintegration process was observed. The images of the disintegration process were recorded through a smartphone (iPhone 12 plus, Apple).

2.10. Friability test of 3D printed tablets

Tablet friability was determined with an HMK-1601 Tablet Friability Tester (AimSizer Scientific Ltd, China) based on the method described in British Pharmacopoeia. For each determination, ten tablets were weighed on an analytical balance with 0.01 mg accuracy before placing in the friability apparatus operated at 25 rpm for 4 min. Afterward, all the tablets were taken out, carefully blown to remove the adhering particles, and accurately weighted. The ratio of weight loss after rotation was calculated by $\frac{W_1-W_2}{W_1} \times 100\%$, where W_1 and W_2 are the pre-test and post-test weights of the total tablets, respectively.

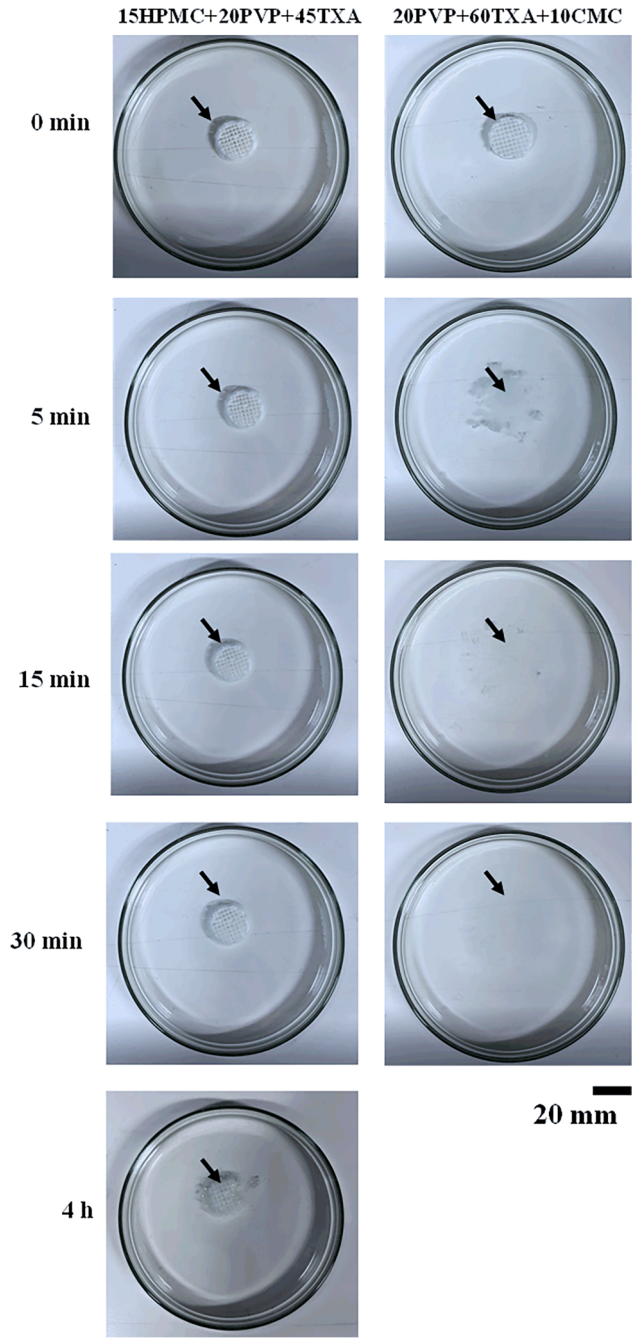

Fig. 6. The disintegration test of the SSE 3D printed tablets (the black arrow shows the changing of the 3D printed tablets with the time).

2.11. *In vitro drug release studies*

Two dissolution media were used, pH 1.2 HCl and pH 6.8 buffer. The pH 1.2 HCl medium was prepared by adding 100 mL of 1 M HCl solution into 1000 mL Milli-Q water and stirring until it completely mixed. For the pH 6.8 buffer medium, 6.8 g of monobasic potassium phosphate (KH_2PO_4) was dissolved in Milli-Q water and diluted with water to 1000 mL in a volumetric flask then stirred for at least 3 h to make sure KH_2PO_4 was completely dissolved. 0.9 g of sodium hydroxide (NaOH) was then added into the solution and stirred for 3 h until completely dissolved. The pH of the result solution was measured using a pH meter (Hanna Instruments, Padova, Italy) and adjusted (if required) to pH 6.8.

The *in vitro* drug release behaviours of the drug-loaded constructs were tested in a Caleva 8ST USP basket dissolution apparatus (Caleva Ltd., Dorset, United Kingdom). The 3D printed tablets were placed in 900 mL dissolution medium either at pH 1.2 HCl or pH 6.8 PBS with 100 rpm paddle rotation rate and at 37 ± 0.5 °C. 5 mL aliquots were withdrawn from the dissolution medium at predetermined time points and replaced with 5 mL of preheated fresh dissolution medium. Sink conditions were maintained during the drug release period. Salicylaldehyde (SA) was used as reagent for the HPLC detection of TXA drug (Mohamed et al., 2015). 1.2 mL of drug solution was added to 1 mL of 1 % (w/v) salicylaldehyde solution (SA). The complete reaction was attained after 12 h.

For the high-performance liquid chromatography (HPLC) measurement of the model drug concentration, an Agilent HPLC system (Palo Alto, CA, USA), equipped with a UV–Visible detector and auto sampler was used. 20 μL of analyte was injected in all experiments. Chromatographic conditions were optimized on a Merck C 18 column (250 × 4.6 mm, 5 μm) and the mobile phase was prepared by mixing methanol-acetate buffer 0.1 mol (75:25, v/v), pH 4 (adjust with acetic acid). The mobile phase flow rate was set as 1.0 mL/min and all the chromatographic work was performed at 25 °C. The UV detection was carried out at 422 nm for TXA drug and 318 nm for IND drug. The retention time of TXA in pH 1.2 HCl and pH 6.8 PBS was found to be 5.2 min, while the retention time of IND in pH 1.2 HCl and pH 6.8 PBS was found to be 8.6 min.

The drug release experiments were performed in triplicate for each construct design. Numerical data were expressed as the mean ± standard deviation and analysed via Student's *t*-test to determine the differences among the groups. Statistical significance is indicated if p-values ≤ 0.05 represents as (*), ≤0.01 as (**), ≤0.001 as (***); while no significance if p-value >0.05.

3. Results and discussion

3.1. *SSE ink development and characterisation of SSE 3D printed tablets*

The viscosity of the HPMC based inks was evaluated by steady-state shear viscosity measurements (Fig. 4a–c). Table 2 summarises the low-shear viscosity of the formulated inks and the results of the printability investigation. It was noted that the filament formation was highly correlated to the viscoelastic properties of the ink, which agreed well with the literature (Zhang et al., 2021a; Zhang et al., 2022). For instance, 15HPMC + 20PVP failed to extrude due to its high viscosity while 15LHPMC + 20PVP was not able to form a filament shape due to its lower viscosity and high flowability. However, it is worthy pointing out that the viscosity of the ink is not the only factor influencing the printability when considering printing multi-layer constructs that have satisfactory shape fidelity after printing. Other rheological parameters such as ink viscoelastic property recovery after experiencing a high shear rate through the printing nozzle could be also important. As an example, although 10HPMC + 25PVP ink has a relatively high viscosity, the printed multi-layer (5-layer) tablets werenot able to hold the structure well, thus it is classified as not printable ink formulation. It is unclear the cause of this, but this could be due to the poor recovery of the viscoelasticity of the ink after extruded out from the nozzle. After adding 45 %w/v TXA in the HPMC based inks, the ink viscosity significantly dropped ($p \leq 0.05$), as shown in Fig. 4a–c. As TXA has an aqueous solubility of 167 mg/mL, 45 %w/v of TXA can be completely dissolved into the HPMC based inks. The drug loaded inks had 45 % w/v of the polymer in the placebo formulation being replaced by TXA solution, which is likely to be the main cause of the viscosity reduction observed.

In our study, four inks, 15HPMC + 20PVP + 45TXA, 15LHPMC + 20PVP + 45TXA, 10HPMC + 25PVP + 45TXA and 20PVP + 10CMC + 60TXA, were used to print 18-layer circular structures. However, the 3D printed constructs using 15LHPMC + 20PVP + 45TXA and 10HPMC + 25PVP + 45TXA had sagging issues, and the 3D printed pores were fully

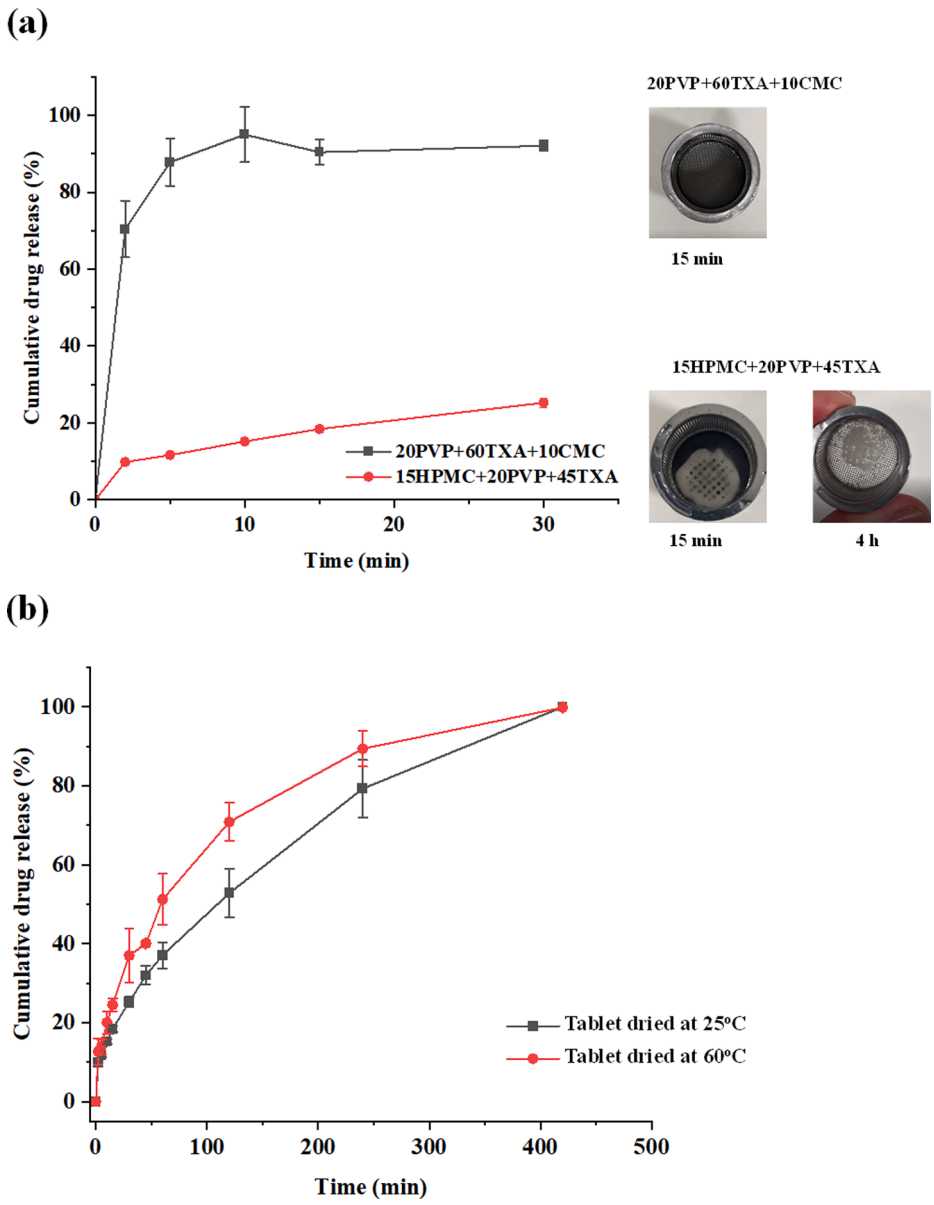

Fig. 7. (a) Drug release data of SSE 3D printed tablets of 15HPMC + 20PVP + 45TXA and 20PVP + 60TXA + 10CMC; (b) The influence of drying temperature on drug release of 15HPMC + 20PVP + 45TXA tablet (n = 3).

closed, as shown in Fig. 4d. This is possibly due to the low molecular weight of LHPMC in the 15LHPMC + 20PVP + 45TXA ink and low polymer concentration in the 10HPMC + 25PVP + 45TXA ink, which led to their low viscosities and high tendencies of flow/spreading after extrusion from the printing nozzle. Thus, only 15HPMC + 20PVP + 45TXA and 20PVP + 10CMC + 60TXA 3D printed tablets were taken for further investigation.

The drying process of the 15HPMC + 20PVP + 45TXA tablet was investigated at three temperatures (25 °C, 37 °C and 60 °C). As shown in Fig. 5a, the rate of weight decrease increases with increasing temperature but after 15 h the final weight remains the same. There is no significant difference for tablets dried at 25 °C, 37 °C and 60 °C in the tablet's dimensions (both diameter and thickness). Fig. 5b and c shows the filament width and pore area values of tablets after drying under different temperatures. Filament width at 25 °C is wider (Fig. 5b), and the pore area is smaller compared to samples dried at 37 °C and 60 °C drying. This is possibly due to a quicker drying speed at higher temperature. The 3D printed structure had more time for viscous flow at ambient temperature (i.e., 25 °C), which led to higher degree of spreading of the filaments and the sagged appearance of the 3D printed structures (Fig. 5d).

The behaviour of drug release is primarily influenced by the disintegration and dissolution behaviour of the drug tablet. The disintegration process is specifically critical for immediate-release dosage forms (Markl and Zeitler, 2017). The rapid dissolving and disintegration of TXA based tablets can ensure the quick release of TXA for anti-bleeding purposes. The disintegration time of SSE 3D printed tablets was quantified by immersing the printed tablets in a Petri dish using a limited volume of liquid resembling more static conditions in the mouth. A similar method was reported by (Conceição et al., 2019). The tablets of 20PVP + 10CMC + 60TXA required less than 5 min, whereas 15HPMC + 20PVP + 45TXA tablets only disintegrated after 7 h in the Petri dish (Fig. 6). One reason 20PVP + 10CMC + 60TXA has much faster disintegration is because of the addition of CMC which is commonly used as a super disintegrant in pharmaceutical formulations (Alqahtani et al., 2020). Another reason is because there is no HPMC involved in the

Table 3
3D printed tablet dimensions.

	Tablet diameter (mm)	Tablet thickness (mm)	Tablet weight (mg)	Drug amount (mg)
SSE 3D printed tablet dimension				
Theoretical dimension	20	5.4		
15HPMC + 20PVP + 45TXA	17.36 ± 0.47	4.71 ± 0.11	481.60 ± 6.25	270.11 ± 2.16
20PVP + 60TXA + 10CMC	17.81 ± 0.43	4.94 ± 0.13	492.30 ± 2.68	328.40 ± 1.79
FDM 3D printed tablet dimension				
Theoretical dimension	20	1		
10 % infill	20.02 ± 0.02	1.05 ± 0.02	116.10 ± 10.9	11.61 ± 1.09
30 % infill	20.04 ± 0.04	0.99 ± 0.02	197.40 ± 3.2	19.74 ± 0.32
Combi-pill (SSE + FDM printed) dimension				
Theoretical dimension	20	7		
Combi pill	20.14 ± 0.15	6.72 ± 0.19	940.10 ± 11.1	19.74 ± 0.32 (IND) 497.72 ± 10.24 (TXA)

20PVP + 10CMC + 60TXA formulation. The presence of HPMC slows the disintegration as although it is soluble it tends to form a gel in water unless actively dispersed, it is often used in solid oral dosage forms as a binder and a controlled-release matrix (Sekharan et al., 2011; Zhang et al., 2021d). According to the British Pharmacopoeia, orodispersible tablets should disintegrate within 15 min. Therefore, 20PVP + 10CMC + 60TXA tablets meet the requirements for orodispersible formulations, but not 15HPMC + 20PVP + 45TXA tablets.

In vitro dissolution tests were carried out within pH 6.8 release medium. Following a similar trend to the disintegration results: 3D printed 20PVP + 60TXA + 10CMC tablets completed TXA drug release in less than 15 min (Fig. 7a), while it took 7 h to reach 100 % drug release from 15HPMC + 20PVP + 45TXA tablets. For example, 20PVP + 60TXA + 10CMC and 15HPMC + 20 PVP + 45 TXA tablets led to 95.9 %± 5.2 % and 17.8 %±0.5 % TXA released respectively in 15 min. The tablet weights of 15HPMC + 20PVP + 45TXA and 20PVP + 60TXA + 10CMC are similar: 491.60 ± 6.25 mg and 492.30 ± 2.68 mg, respectively. As shown in Table 3, the TXA weight per tablet is 270.11 ± 2.16 and 328.40 ± 1.79 for tablets of 15HPMC + 20 PVP + 45 TXA and 20PVP + 60TXA + 10CMC, respectively. In spite of the weight difference both of tablets were tested under sink conditions. As described earlier CMC disintegrant should facilitate the rapid breakdown of tablets into small fragments, resulting in faster dissolution and rapid drug release (Alqahtani et al., 2020; Kumar and Kumari, 2019). The influence of drying temperature influence on *in vitro* drug dissolution tests was performed. As shown in Fig. 7b, the drug release rate of tablets drying at 60 °C is slightly higher than the one drying at 25 °C. One of the possible reasons as mentioned previously is that the pore area of the tablets drying at 60 °C is slightly bigger than that at 25 °C (Fig. 5b). Other studies (Zhang et al., 2021c; Zhang et al., 2021e) also showed that drug release rate increased with increasing pore area as larger pore surface areas result in faster transfer rates into solution.

3.2. HME filament development and characterisation of FDM printed tablets

The FDM printed tablet was based on Eudragit RL, but the extruded filament from Eudragit RL and IND binary formulation was too fragile for FDM printing. The addition of plasticizers were shown to improve the elasticity of the filament and increase the mechanical suitability of a filament for FDM (Nasereddin et al., 2018; Alhijjaj et al., 2019). Therefore, the Eudragit RL/IND/plasticizers filaments formulated in this study contained 10, 10, and 20 % (w/w) of Tween 80, PEG 4000 and PEO, respectively, as plasticizers to improve the printability of the filaments. Fig. 8a show the force–displacement analysis of the Eudragit RL/IND/plasticizers filaments. The fractured point of the filament was not at the points contacted by the grips but between the grip points, thus the fracture points were within the measurement region. The Eudragit RL/IND/plasticizers filaments yield strength was 20.86 ± 1.31 Pa and the fracture strength was 27.96 ± 1.81 Pa, thus they were able to sustain the force experienced during the FDM feeding and printing.

ATR-FTIR was carried out to investigate any possible molecular interactions among the polymer, plasticizers and drug. Fig. 8b shows the ATR-FTIR spectra of Eudragit RL, PEO, PEG 4000 and Tween 80, as well as the physical mix, the Eudragit RL/IND/plasticizers filaments prepared by HME and FDM printed IND tablet. The PEO and PEG 4000 peaks at 1341 cm^{-1}, 1077 cm^{-1} and 2876 cm^{-1} correspond to C—H, O—H bending and C—H stretching. The Eudragit RL peaks at 1750 cm^{-1} represents a C═O stretch, which is visibly unchanged in the HME filaments and FDM tablet indicating no specific interactions between Eudragit RL, PEG 4000 and PEO. The IND peak at 1668 cm^{-1} is a C═O stretch and the peaks at 1662 cm^{-1} and 1639 cm^{-1} are ring deformations (Badawi and Förner, 2014). The simulated spectrum of the physical mix, using the spectra of individual ingredients with normalized intensities shows a clear match with the measured physical mix, indicating no significant change of the physical states of the drug and excipients in the physical mixes. In the spectra of HME filaments and FDM printed tablets, changes in peak intensities are particularly noticeable in the 1000–1200 cm^{-1} region in which the C—O stretching peaks are much more intense than the ones in the physical mix spectra. This intensity arises largely from PEG and PEO. Since ATR-FTIR is essentially a surface technique having a typical penetration depth of about 1 μm it may be assumed that the processing results in a layer of these polymers on, or close to, the surface. In the carbonyl region (1640–1780 cm^{-1}) the intensity in the sample closely resembles the physical mix spectrum. However, in the tablet sample there is a shoulder centred around 1760 cm^{-1} that is not present in the physical mix spectrum or any of the components. The origin of this is not clear but it does suggest that in the FDM tablet, at least on the surface, there has been a change in the hydrogen bonding pattern as result of the 3D printing process.

The FDM tablets dimensions are shown in Table 3. By keeping the tablet diameter (20 mm) and thickness (1 mm) constant, 30 % infill and 10 % infill FDM tablets have the theoretical pore widths of 1 mm and 3.8 mm, respectively. The influence of infill (or pore width) on the drug release rate of IND tablets were investigated. As shown in Fig. 9a, the constructs with a pore width of 3.8 mm (10 % infill), more than 12 % of the drug was released within the first 120 min (Fig. 9b). In contrast, only about 3.5 % of the drug was released from the samples with pore width of 1 mm (30 % infill). At 2400 min, the drug release rates were 55.17 % ± 2.37 % and 27.34 % ± 0.61 % for the 3D printed samples of 10 % infill and 30 % infill, respectively. The theoretical surface area to volume (SA/V) ratio of 30 % infill and 10 % infill are respectively 9.01 and 8.32, which were calculated based on the Equation (1). Although SA/V of 10 % infill is slightly higher than 30 % infill, the ratio of the SA/V values between them is about 1:1. This implies that the change in drug release

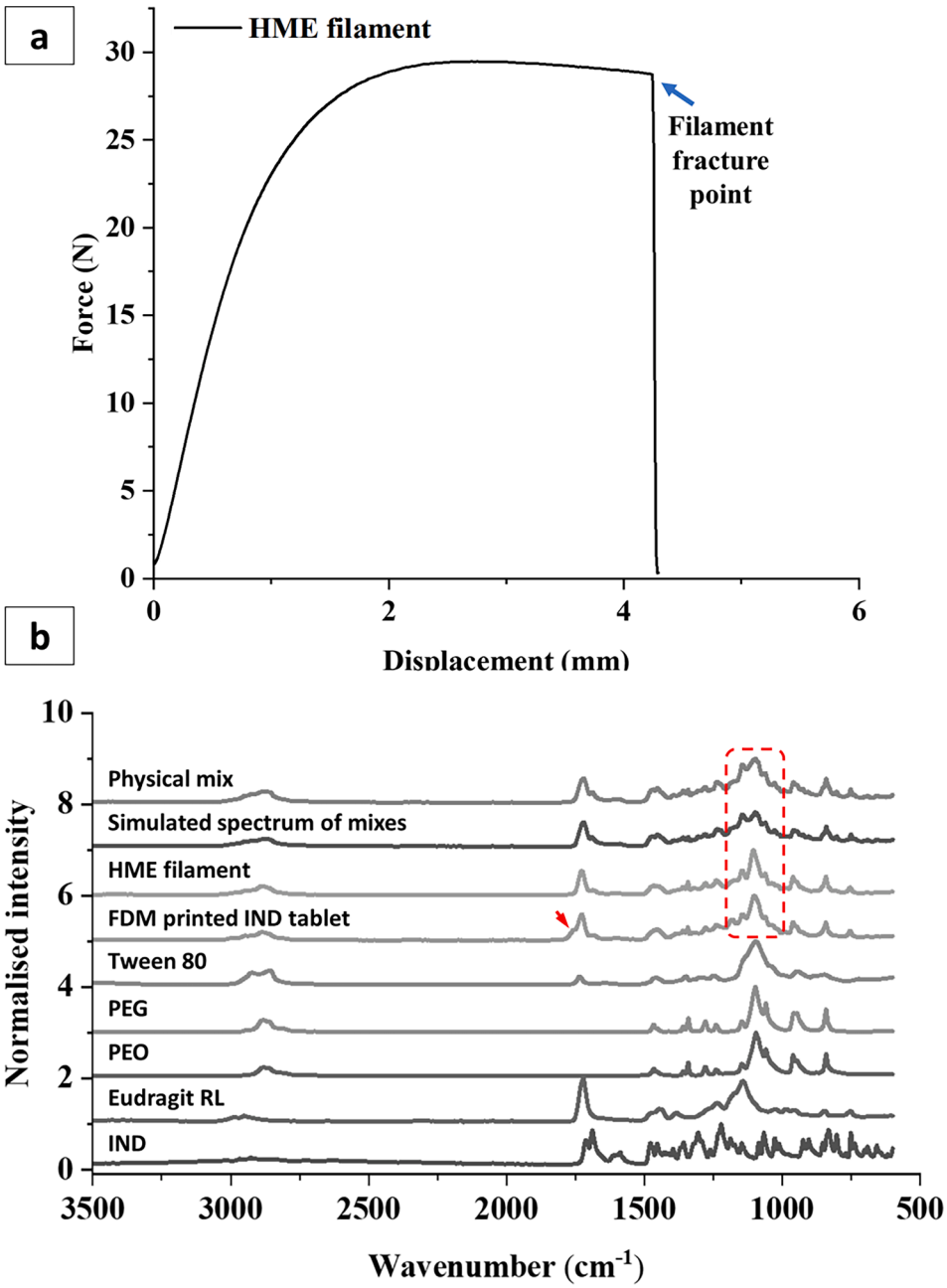

Fig. 8. (a) Texture analysis profile of Eudragit RL/IND/plasticizers HME filaments for FDM printing (n = 3); (b) ATR-FTIR of the raw materials, the physical mix, Eudragit RL/IND/plasticizers HME filaments and FDM tablet.

rate is not related to the SA/V. The drug release rate increased with increasing pore width in both pH 1.2 HCl and pH 6.8 PBS. This can be attributed to the drug needing to diffuse through multiple extruded filaments, rather than to the surface of a single extruded filament. The drug release of the sample with smaller pore width would release more quickly by diffusion in comparison to the one with larger pores, this finding is in line with other studies (Zhang et al., 2021b; Zhang et al., 2021c; Mcdonagh et al., 2022).

3.3. Characterisation of 3D printed combi-pills

The combi-pill was fabricated using both FDM and SSE techniques. The SSE printed TXA tablet was located on top of the FDM printed IND tablet. Fig. 10a shows the 3D combi-pill. The SEM images of longitudinal and transversal cross-sections of combi-pills were observed, as shown in Fig. 10b. The transversal cross-sections of single TXA and IND tablet are shown in Fig. 10c. The TXA tablet layer adhered well to the IND tablet layer and required a blade to separate the two layers.

TXA is zwitterionic (Groth, 1968). The assignment of the IR bands of crystalline TXA must therefore take account of the transfer of a proton from the carbonyl group to the amino group. Assignment therefore must be based on this structure rather than a simple amino structure as has been done previously (Muthu and Prabhakaran, 2014). As seen in Fig. 11, the ATR-FTIR spectra of the TXA + IND combi-pill interface between the TXA and IND layers were compared with the spectra of the surfaces of the SSE printed TXA tablets and FDM printed IND tablets. There is a strong cluster of peaks in the region 3000 to 2500 cm^{-1} representing both $NH3^{+}$ and CH vibrational modes of TXA. There are

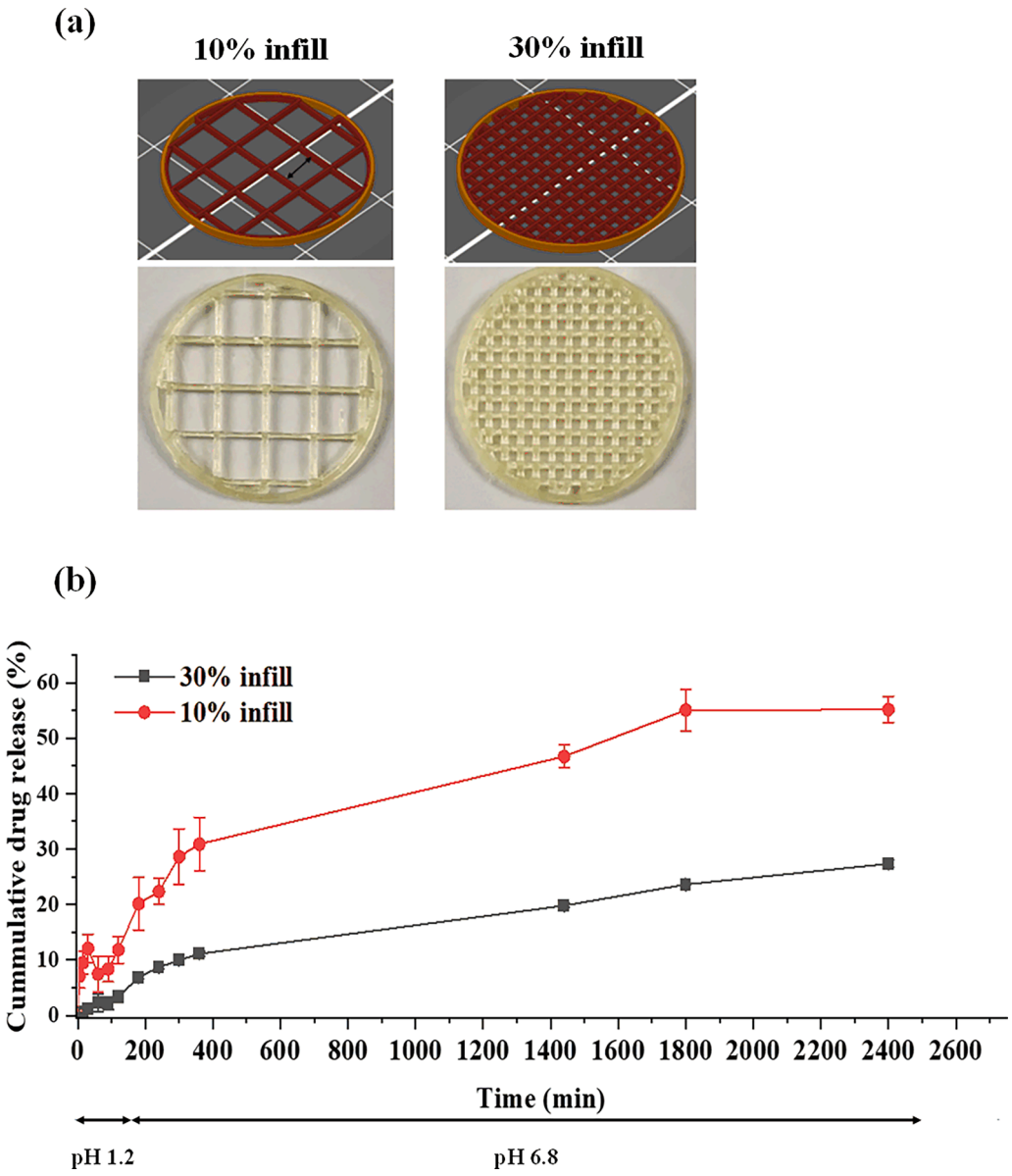

Fig. 9. (a)The FDM tablet with the infill of 10 % and 30 %; (b) Drug release data of FDM tablets (n = 3); the dissolution in the first 120 min was implemented in the buffer with pH 1.2 which was changed to pH 6.8 from 120 min onwards.

also strong peaks at 1533 and 1376 cm^{-1} arising from C═O of TXA which are also not present in the IND spectrum. A strong doublet around 1700 cm^{-1} from C═O and peaks at 1210 and 995 cm^{-1} from aromatic CH of IND and only exist in the FDM printed IND tablets. When the interface of two layers were examined, as seen in Fig. 11, the characteristic peaks of IND at 1700 cm^{-1} and TXA at 1690 cm^{-1} and 1533 cm^{-1} can be clearly observed in the spectra of both the surfaces of TXA layer in contact with the IND layer (with high TXA peak intensity and low IND peak intensity) and the surfaces of IND layer in contact with the TXA layer (with high IND peak intensity and low TXA peak intensity). This indicates the penetration of the drug molecules into the neighbouring layer. This is likely to be caused by the diffusion of solvents in the SSE ink into the FDM printed solid layer during drying. As this is expected to be limited to the surface layer of the IND print in small amounts, it is not expected to affect the overall release rate of the TXA.

Friability testing is commonly used to test the durability of tablets during packing processes and transit (Abebe et al., 2020). Based on the specification of British Pharmacopeia, it should take a sample of 10 whole tablets for tablets with a unit mass of more than 650 mg. After the friability tests, there was no cracked, cleaved or broken tablets were found. The weight loss percentage for combi-pill tablets post friability test is 0.75 ± 0.09 %, which met the no more than 1 % weight loss of the specification of British Pharmacopeia (Deshpande et al., 2011).

For the combi-pills, the IND and TXA drug load per combi-pill are 19.74 ± 0.32 mg and 497.72 ± 10.24 mg, respectively, which are the recommended dosage for commercialised tablets of IND (20 mg per tablet) and TXA (500 mg per tablet) (Yeh, 1985; Dunn and Goa, 1999). The TXA and IND release profiles from the combi-pills are shown in Fig. 12. The TXA layer released 100 % TXA within 15mins in pH 1.2 HCl, while IND only released about 8 % from the sustained release layer after the first 2 h. The IND layer continued to release IND after the change of media to pH 6.8 PBS to mimic the transition from gastric to intestinal pH and reached about 29.30 % ± 3.33 % at 46 h. As shown in Fig. 12b, the error bars of the TXA release data are larger than the ones of IND release data. This could be due to the variations in the fast disintegration and delamination of the TXA layer from the combi-pill. The drug release data

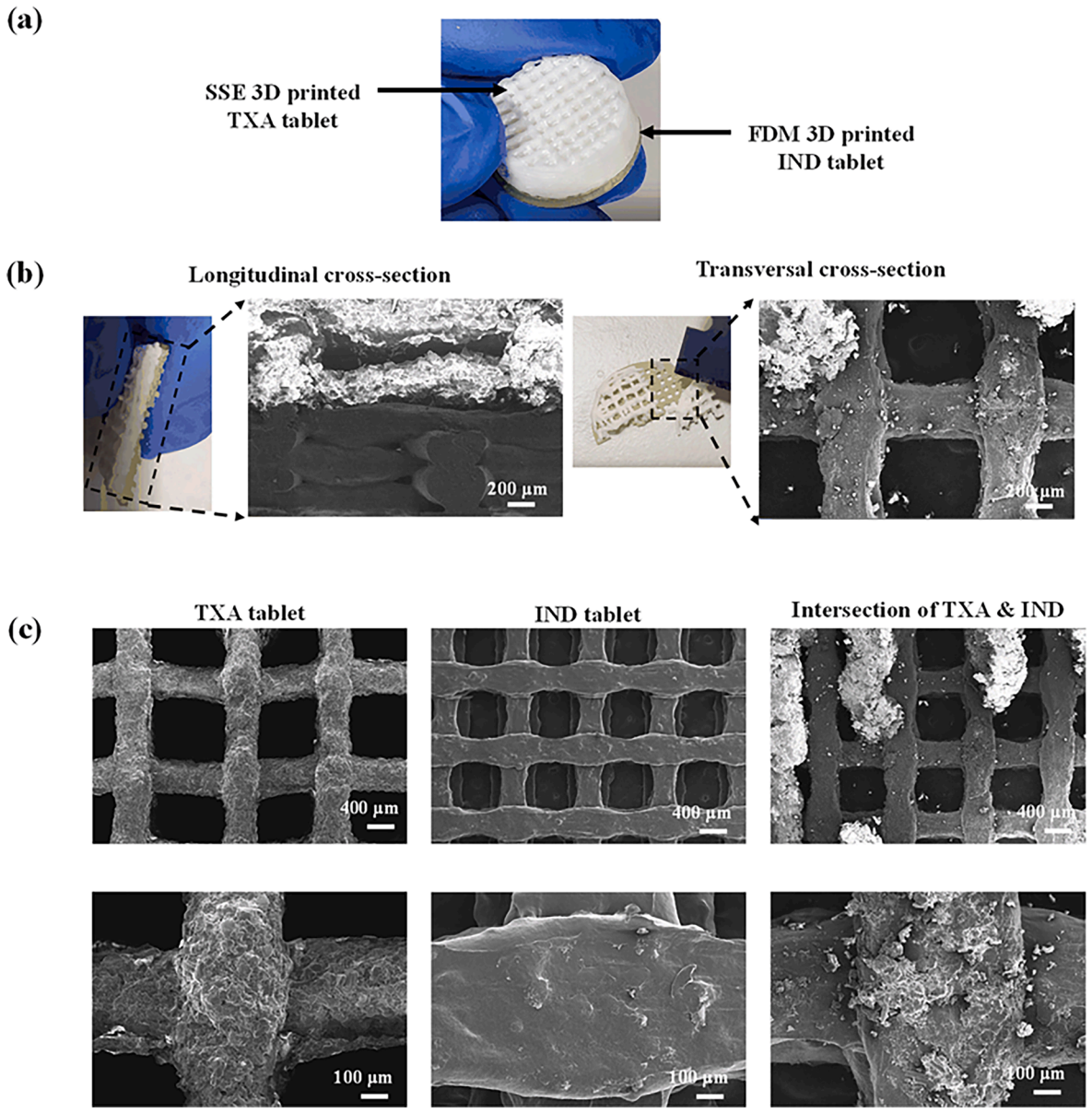

Fig. 10. (a) 3D combi-pill; (b)The SEM image of longitudinal and transversal cross-section from the combi-pill; (c) SEM images of transversal cross-section from single TXA, IND and combi-pill.

demonstrated the clear separation of drug release profiles of the intended fast and sustained release of the two model drugs. This result confirmed the potential of combined use of SSE and FDM 3D printing for manufacturing combi-pills with the capability of delivering different drugs and well-controlled pre-programmed release kinetics.

4. Conclusions

In this study, the combined use of SSE and FDM 3D printing to produce combi-pills with distinctly different drug release kinetics was investigated and demonstrated. TXA loaded semisolid SSE inks were optimised for SSE 3D printed tablets. It was demonstrated that the use of matrix polymer can significantly affect the drug release kinetics and change the immediate release to sustained release by the addition of HPMC. A clear relationship between the low shear viscosity of the SSE ink and their printability was observed. The high dose TXA ink had significantly lower viscosity than the placebo of HPMC-based SSE inks. FDM 3D printing IND tablet was developed with a sustained release profile. For the first time, a TXA + IND combi-pill, incorporated TXA at the top layer and IND in the bottom layer, fabricated by two different 3D printing methods were produced and tested. The bi-layered combi-pills passed BP friability specifications and achieved dual-release profiles with 100 % release of TXA within the first 15 min and sustained drug release of IND of less than 30 % in 46 h. This *in vitro* dual-release kinetics meant that the combi-pill could achieve rapid antibleeding and prolonged anti-inflammation therapeutic indications with the use of one tablet. This study developed a new combined 3D printing methodology to manufacture combi-pills with dual drug release kinetics. The insights from the ink and filament developments can also be used as practical design guidance for the controlled performance of extrusion-based 3D printed porous materials for personalised pharmaceuticals.

Declaration of Competing Interest

The authors declare that they have no known competing financial interests or personal relationships that could have appeared to influence the work reported in this paper.

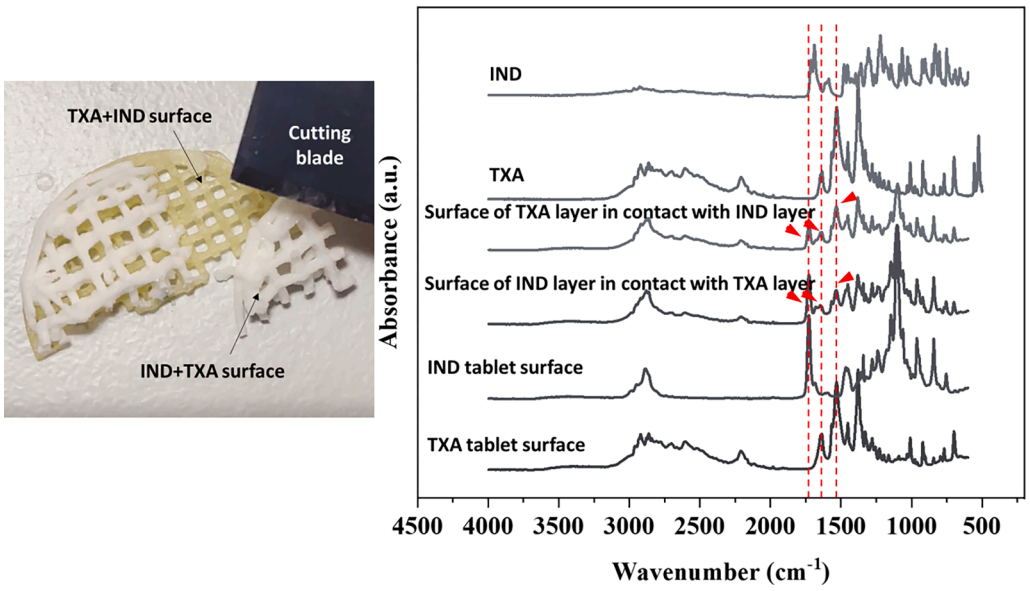

Fig. 11. Photo of a combi-pill with the surfaces between the top layer of TXA tablet and bottom layer of IND tablet being separated by a blade (left), and the ATR-FTIR spectra (right) of crystalline TXA, IND, the surfaces of TXA and IND tablets, and the surfaces of the TXA layer (the surface that IND contacted with TXA surface), and the IND layer (the surface that TXA contacted with IND surface) that were separated from a combi-pill.

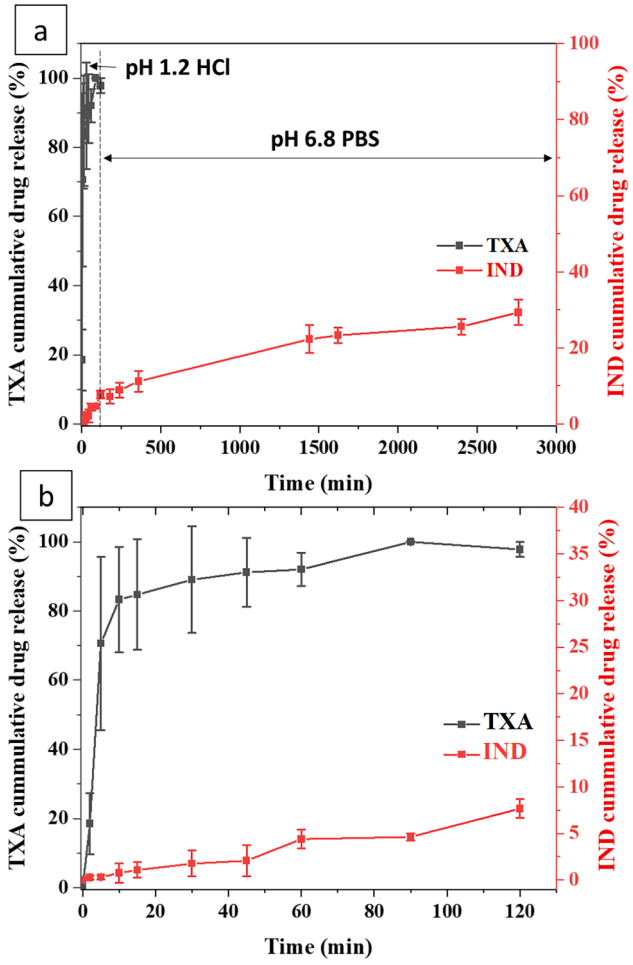

Fig. 12. Drug release profiles of TXA and IND from the combi-pills (a) in pH 1.2 HCl (first 120 min) and pH 6.8 PBS (120 min onwards); (b) the drug release within the first 120 min in pH 1.2 HCl. The formulation compositions of the TXA and IND tablet layers of the combi-pill are 20PVP + 15CMC + 45TXA and 50Eudragit RL/10IND/40plasticisers (plasticiser ratio of Tween 80:PEG 4000: PEO being 10:10:20), respectively.

Data availability

Data will be made available on request.

Acknowledgements

This research was funded by the Redistributed Manufacturing in Healthcare Network (RiHN). The RiHN was awarded a grant from the UK Engineering and Physical Sciences Research Council (EPSRC) (Ref. EP/T014970/1).

References

Abebe, K., Beressa, T.B., Yimer, B.T., 2020. In-vitro evaluations of quality control parameters of paracetamol tablets marketed in Gondar City, Northwest Ethiopia. Drug Healthcare Patient Saf. 12, 273.

Alhijjaj, M., Belton, P., Qi, S., 2016. An investigation into the use of polymer blends to improve the printability of and regulate drug release from pharmaceutical solid dispersions prepared via fused deposition modeling (FDM) 3D printing. Eur. J. Pharm. Biopharm. 108, 111–125.

Alhijjaj, M., Nasereddin, J., Belton, P., Qi, S., 2019. Impact of processing parameters on the quality of pharmaceutical solid dosage forms produced by fused deposition modeling (FDM). Pharmaceutics 11, 633.

Alqahtani, F., Belton, P., Zhang, B., Al-Sharabi, M., Ross, S., Mithu, M.S.H., Douroumis, D., Zeitler, J.A., Qi, S., 2020. An investigation into the formations of the internal microstructures of solid dispersions prepared by hot melt extrusion. Eur. J. Pharm. Biopharm.

Auriemma, G., Tommasino, C., Falcone, G., Esposito, T., Sardo, C., Aquino, R.P., 2022. Additive manufacturing strategies for personalized drug delivery systems and medical devices: fused filament fabrication and semi solid extrusion. Molecules 27, 2784.

Azad, M.A., Olawuni, D., Kimbell, G., Badruddoza, A.Z.M., Hossain, M., Sultana, T., 2020. Polymers for extrusion-based 3D printing of pharmaceuticals: a holistic materials–process perspective. Pharmaceutics 12, 124.

Badawi, H.M., Förner, W., 2014. Analysis of the molecular structure and vibrational spectra of the indole based analgesic drug indomethacin. Spectrochim. Acta A: Mol. Biomol. Spectrosc. 123, 447–454.

Baumgartner, A., Drame, K., Geutjens, S., Airaksinen, M., 2020. Does the polypill improve patient adherence compared to its individual formulations? A systematic review. Pharmaceutics 12, 190.

Conceição, J., Farto-Vaamonde, X., Goyanes, A., Adeoye, O., Concheiro, A., Cabral-Marques, H., Lobo, J.M.S., Alvarez-Lorenzo, C., 2019. Hydroxypropyl-β-cyclodextrin-based fast dissolving carbamazepine printlets prepared by semisolid extrusion 3D printing. Carbohydr. Polym. 221, 55–62.

Crossan, C., Dehbi, H.-M., Williams, H., Poulter, N., Rodgers, A., Jan, S., Thom, S., Lord, J., 2018. A protocol for an economic evaluation of a polypill in patients with established or at high risk of cardiovascular disease in a UK NHS setting: RUPEE (NHS) study. BMJ Open 8, e013063.

Deshpande, R.D., Gowda, D., Mahammed, N., Maramwar, D.N., 2011. Bi-layer tablets-An emerging trend: a review. Int. J. Pharm. Sci. Res. 2, 2534.
Dunn, C.J., Goa, K.L., 1999. Tranexamic acid. Drugs 57, 1005–1032.
Goyanes, A., Wang, J., Buanz, A., Martínez-Pacheco, R., Telford, R., Gaisford, S., Basit, A. W., 2015. 3D printing of medicines: engineering novel oral devices with unique design and drug release characteristics. Mol. Pharm. 12, 4077–4084.
Group, P.C., 2011. An international randomised placebo-controlled trial of a four-component combination pill ("polypill") in people with raised cardiovascular risk. PLoS ONE 6, e19857.
Groth, P., 1968. Crystal structure of the trans form of 1, 4-aminomethylcyclohexane-carboxylic acid. Acta Chem. Scand. 22.
Haring, A.P., Tong, Y., Halper, J., Johnson, B.N., 2018. Programming of multicomponent temporal release profiles in 3D printed polypills via core–shell, multilayer, and gradient concentration profiles. Adv. Healthcare Mater. 7, 1800213.
Hsiao, W.-K., Lorber, B., Reitsamer, H., Khinast, J., 2018. 3D Printing of Oral Drugs: A New Reality or Hype? Taylor & Francis.
Huebner, B.R., Dorlac, W.C., Cribari, C., 2017. Tranexamic acid use in prehospital uncontrolled hemorrhage. Wilderness Environ. Med. 28, S50–S60.
Khaled, S.A., Burley, J.C., Alexander, M.R., Yang, J., Roberts, C.J., 2015. 3D printing of five-in-one dose combination polypill with defined immediate and sustained release profiles. J. Control. Release 217, 308–314.
Kumar, R.S., Kumari, A., 2019. Superdisintegrant: crucial elements for mouth dissolving tablets. J. Drug Del. Therapeut. 9, 461–468.
Markl, D., Zeitler, J.A., 2017. A review of disintegration mechanisms and measurement techniques. Pharm. Res. 34, 890–917.
McDonagh, T., Belton, P., Qi, S., 2022. An investigation into the effects of geometric scaling and pore structure on drug dose and release of 3D printed solid dosage forms. Eur. J. Pharm. Biopharm.
Mohamed, G.G., Frag, E.Y., Sedeek, A.A., 2015. Spectrophotometric methods for determination of tranexamic acid and etamsylate in pure form and pharmaceutical formulation. Insight Pharm. Sci. 5, 1–7.
Muñoz, D., Uzoije, P., Reynolds, C., Miller, R., Walkley, D., Pappalardo, S., Tousey, P., Munro, H., Gonzales, H., Song, W., 2019. Polypill for cardiovascular disease prevention in an underserved population. N. Engl. J. Med. 381, 1114–1123.
Muthu, S., Prabhakaran, A., 2014. Vibrational spectroscopic study and NBO analysis on tranexamic acid using DFT method. Spectrochim. Acta Part A Mol. Biomol. Spectrosc. 129, 184–192.
Nalamachu, S., Wortmann, R., 2014. Role of indomethacin in acute pain and inflammation management: a review of the literature. Postgrad. Med. 126, 92–97.
Nasereddin, J.M., Wellner, N., Alhijjaj, M., Belton, P., Qi, S., 2018. Development of a simple mechanical screening method for predicting the feedability of a pharmaceutical FDM 3D printing filament. Pharm. Res. 35, 151.
Pereira, B.C., Isreb, A., Forbes, R.T., Dores, F., Habashy, R., Petit, J.-B., Alhnan, M.A., Oga, E.F., 2019. 'Temporary Plasticiser': a novel solution to fabricate 3D printed patient-centred cardiovascular 'Polypill' architectures. Eur. J. Pharm. Biopharm. 135, 94–103.
Reardon, S., 2011. Experts Debate Polypill: A Single Pill for Global Health. American Association for the Advancement of Science.
Robles-Martinez, P., Xu, X., Trenfield, S.J., Awad, A., Goyanes, A., Telford, R., Basit, A. W., Gaisford, S., 2019. 3D printing of a multi-layered polypill containing six drugs using a novel stereolithographic method. Pharmaceutics 11, 274.
Roshandel, G., Khoshnia, M., Poustchi, H., Hemming, K., Kamangar, F., Gharavi, A., Ostovaneh, M.R., Nateghi, A., Majed, M., Navabakhsh, B., 2019. Effectiveness of polypill for primary and secondary prevention of cardiovascular diseases (PolyIran): a pragmatic, cluster-randomised trial. The Lancet 394, 672–683.
Sekharan, T.R., Palanichamy, S., Tamilvanan, S., Shanmuganathan, S., Thirupathi, A.T., 2011. Formulation and evaluation of hydroxypropyl methylcellulose-based controlled release matrix tablets for theophylline. Ind. J. Pharm. Sci. 73, 451.
Tamargo, J., Castellano, J.M., Fuster, V., 2015. The fuster-CNIC-ferrer cardiovascular polypill: a polypill for secondary cardiovascular prevention. Int. J. Cardiol. 201, S15–S23.
Tan, D.K., Maniruzzaman, M., Nokhodchi, A., 2018. Advanced pharmaceutical applications of hot-melt extrusion coupled with fused deposition modelling (FDM) 3D printing for personalised drug delivery. Pharmaceutics 10, 203.
Thom, S., Field, J., Poulter, N., Patel, A., Prabhakaran, D., Stanton, A., Grobbee, D.E., Bots, M.L., Reddy, K.S., Cidambi, R., 2014. Use of a multidrug pill in reducing cardiovascular events (UMPIRE): rationale and design of a randomised controlled trial of a cardiovascular preventive polypill-based strategy in India and Europe. Eur. J. Prevent. Cardiol. 21, 252–261.
Wald, D.S., Morris, J.K., Wald, N.J., 2012. Randomized polypill crossover trial in people aged 50 and over.
Wening, K., Breitkreutz, J., 2011. Oral drug delivery in personalized medicine: unmet needs and novel approaches. Int. J. Pharm. 404, 1–9.
Yeh, K.C., 1985. Pharmacokinetic overview of indomethacin and sustained-release indomethacin. Am. J. Med. 79, 3–12.
Zhang, B., Chung, S.H., Barker, S., Craig, D., Narayan, R.J., Huang, J., 2020a. Direct ink writing of polycaprolactone/polyethylene oxide based 3D constructs. Prog. Nat. Sci.: Mater. Int.
Zhang, B., Huang, J., Narayan, R., 2020b. Gradient scaffolds for osteochondral tissue engineering and regeneration. J. Mater. Chem. B.
Zhang, B., Chung, S.H., Barker, S., Craig, D., Narayan, R.J., Huang, J., 2021a. Direct ink writing of polycaprolactone/polyethylene oxide based 3D constructs. Prog. Nat. Sci.: Mater. Int. 31, 180–191.
Zhang, B., Teoh, X., Belton, P., Gleadall, A., Bibb, R., Qi, S., 2021d. The development of Hypromellose based semisolid 3D printing inks for drug delivery. Trans. Addit. Manuf. Meets Med. 3, 541.
Zhang, B., Gleadall, A., Belton, P., McDonagh, T., Bibb, R., Qi, S., 2021b. New insights into the effects of porosity, pore length, pore shape and pore alignment on drug release from extrusionbased additive manufactured pharmaceuticals. Addit. Manuf. 46, 102196.
Zhang, B., Nasereddin, J., McDonagh, T., von Zeppelin, D., Gleadall, A., Alqahtani, F., Bibb, R., Belton, P., Qi, S., 2021c. Effects of porosity on drug release kinetics of swellable and erodible porous pharmaceutical solid dosage forms fabricated by hot melt droplet deposition 3D printing. Int. J. Pharm., 120626
Zhang, B., Nguyen, A.K., Narayan, R.J., Huang, J., 2022. Direct ink writing of vancomycin-loaded polycaprolactone/polyethylene oxide/hydroxyapatite 3D scaffolds. J. Am. Ceram. Soc. 105, 1821–1840.
Zhang, B., Gleadall, A., Belton, P., McDonagh, T., Bibb, R., Qi, S., 2021e. New insights into the effects of porosity, pore length, pore shape and pore alignment on drug release from extrusionbased additive manufactured pharmaceuticals. Addit. Manuf. 46, 102196.